# CONTROL LAWS FOR AN ACTIVE TUNABLE VIBRATION ABSORBER DESIGNED FOR ROTOR BLADE DAMPING AUGMENTATION

Fred Nitzsche
Department of Mechanical and Aerospace Engineering
Carleton University, Ottawa, Canada

David. G. Zimcik, Viresh K. Wickramasinghe and Chen Yong
Institute for Aerospace Research
National Research Council Canada, Ottawa, Canada

## ABSTRACT

Most Individual Blade Control (IBC) approaches have attempted to suppress the rotor vibration by actively altering the varying aerodynamic loads on the blade using techniques such as trailing edge servo-flaps or imbedded piezoelectric fibers to twist the blade. Unfortunately, successful implementation of these approaches has been hindered by electromechanical limitations of piezoelectric actuators. The Smart Spring is a unique approach that is designed to suppress the rotor vibration by actively altering the structural stiffness of the blade out of phase with the time varying aerodynamic forces. The Smart Spring system is able to adaptively alter the stiffness properties of the blade while requiring only small deformations of the actuator, which overcomes the major problems inherent in the former approaches. The theoretical characterization of the Smart Spring system as a class of active Tunable Vibration Absorbers (TVA) is presented in the paper. A real-time adaptive control system was developed for a Smart Spring to suppress vibration in a non-rotating blade. Initial aerodynamic wind tunnel test results using the proof-of-concept model of the device in a fixed blade indicate that the Smart Spring can evolve into a powerful approach to IBC.

## INTRODUCTION

Helicopter rotors operate in a highly complex unsteady aerodynamic environment caused by cyclic variation of centrifugal and aerodynamic loads on the rotating blades. Structural vibration due to unsteady aerodynamics is a notable and undesirable characteristic of helicopter flight. Vibratory hub loads are transferred throughout the helicopter structure contributing to poor ride quality for passengers and fatigue of expensive structural components. Suppression of rotor vibration is a matter of continuing investigation around the world.

In additional to passive approaches, such as vibration absorbers or addition of mass to tune blades, active control solutions are currently being investigated to suppress helicopter rotor vibration. The active approaches promise vibration suppression in a broadband of frequencies unlike passive techniques that are typically capable of suppressing vibration over a narrow frequency range. The Individual Blade Control (IBC) approach has been identified as the most promising active vibration suppression methods currently under development. IBC places actuators on the blade to control each blade independently and simultaneously to suppress the vibration at the source [1]. However, conventional servo-hydraulic actuator systems first considered for IBC had important limitations. These limitations include, (a) multiple energy conversions from mechanical to hydraulic to electrical and back to mechanical, (b) large numbers of parts in the system that lead to high probability of failure and (c) low frequency operation of hydraulic systems [2]. Recent advances in smart material actuators have the potential to overcome these limitations of conventional servo-hydraulic actuators. In contrast to servo-hydraulic systems, active material actuator systems offer direct conversion of electrical energy to produce high frequency mechanical motion. Furthermore, these systems have fewer parts compared to conventional systems [3].

In the past, IBC using active material actuators for rotor vibration suppression has been implemented using two distinct actuation concepts, namely, discrete and integral. The discrete actuation concept employs an active material actuator imbedded in the blade to control a trailing edge servo-flap. A 1/6-scale blade with a trailing edge flap based on a "X-Frame" displacement amplification concept, driven by a stacked piezoelectric actuator, was developed and hover tested by Prechtl and Hall [4] and Straub et al. [5]. Unfortunately, the fundamental problem with this approach is the need for complex displacement amplification devices that must be highly robust to operate under the extreme dynamic environment that ex-

ists in the rotor blade. Displacement amplification is essential to obtain the required flap deflection necessary for vibration suppression, from the limited displacement of piezoceramic actuators.

In the integral actuation concept, the actuator system is either embedded or bonded to the skin along the blade span to obtain a smooth continuous structural deformation [6]. Rodgers and Hagood tested a 1/6-scale, Mach-scaled, blade in hover with embedded Active Fiber Composite (AFC) actuators made of piezoceramic fibers for integral actuation [7]. Shin and Cesnik also tested a similar set of AFC embedded Froude-scaled blades [8]. The drawback with this approach is the requirement of very high voltages to induce sufficient actuation from AFCs, which have been operated with 3000 V peak to peak driving voltage cycle to generate the required blade twist for rotor vibration suppression [9].

It is important to note that all of the above IBC approaches for vibration suppression attempted to actively alter the time varying aerodynamic loads on the blade. However, successful implementation of these approaches has been hindered by electromechanical limitations of smart material actuators, specifically piezoceramic actuators, used in these applications. Restricted deformation capabilities of these actuators required complex displacement amplification mechanisms to be implemented or application of extremely high voltages in order to achieve the required vibration suppression performance. The Smart Spring provides a unique approach for IBC that overcomes these difficulties.

This paper describes the concept and design of the Smart Spring for IBC in helicopter rotor vibration suppression. A proof-of-concept hardware model of the Smart Spring has been built and incorporated into a fixed blade for preliminary wind tunnel tests. For the sake of simplicity of hardware construction, in these preliminary wind tunnel tests only the torsion degree of freedom of the blade sought to be actively controlled. The results of this experiment are discussed in the present work.

## THE SMART SPRING CONCEPT

In order to achieve the goal of rotor vibration suppression using IBC in helicopters, it is possible to alter either the time varying loads on each blade, or the stiffness of the blades in response to the variable aerodynamic loads [10]. Most IBC techniques currently under development are designed to control the aerodynamic loads on the blade to suppress rotor vibration. The Smart Spring concept is unique in contrast to other IBC approaches because it is designed to actively alter the blade dynamic stiffness properties to vary the blade response in order to suppress the vibration. Analytical modeling of the Smart Spring concept has demonstrated that active adaptation of dynamic stiffness of the blade boundary condition at the root is an effective approach to suppress the rotor vibration [11].

Basic Concept

The Smart Spring is a patented concept based on an active variable stiffness device that adaptively varies the blade stiffness at the root to suppress vibration [12]. The mechanism, shown in the conceptual drawing in Fig. 1 can be seen as an actively Tunable Vibration Absorber (TVA) that exploits the large stiffness and bandwidth of the piezoelectric materials, while circumventing their lack of power at lower frequencies.
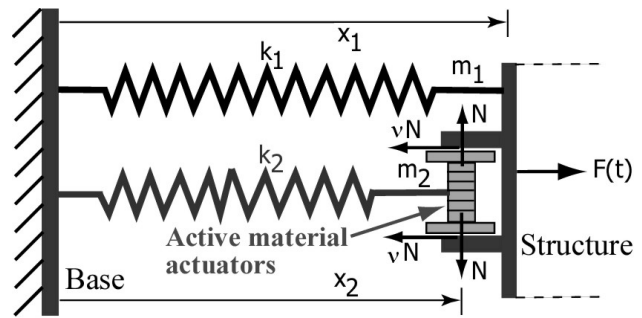


Figure 1: Smart Spring concept

In Fig. 1, two linear springs of constants $k_1$ and $k_2$, respectively, are attached to an axially moving structure and a sleeve that can slide with respect to the structure. An external force $F(t)$ is applied to the structure attached to the spring designated by $k_1$. A stack of piezoelectric actuators is inserted in the sleeve attached to the spring designated by $k_2$. When the actuator is off, the sleeve can move freely and the dynamic response is determined by the single mass-spring system consisting of $m_1$ and $k_1$.

When the actuator is turned on, a normal force $N(t)$ engages the sleeve. If the resultant friction force, $\nu N(t)$ shown in the figure is sufficiently large, the two springs are forced to move together and a combination of two springs in parallel is obtained. Therefore, the stiffness of the system increases from its original value, $k_i = k_1$ to the final value, $k_f = k_1 + k_2$ for two

springs in parallel. In reality, the two limiting conditions of a single spring or two springs in parallel are never achieved since sliding of the sleeve is always present. The dynamic friction force $\nu N(t)$ applied on the sleeve, which can be controlled by an external stimulus, forces the spring designated by $k_2$ into motion. As a result, the voltage applied to the piezoelectric stack can continuously control the total stiffness of the TVA, such that $k_i \leq k(t) \leq k_f$. It is important to understand that the concept relies on delivering power not to actuate against the inertial and aerodynamic loads but only to change the *effective* spring constant of the device. It is this change of the flexural characteristics that will allow the control of the aeroelastic response of the system. Therefore, such a device is able to control aeroelastic response in an *indirect* way.

A schematic of the actuator arrangement is shown in Fig. 1. In fact, any mechanism whose flexural properties can be actively varied using "smart" materials would fall into the class of TVAs under investigation and be called a Smart Spring. For example, in the case of the prototype tested, the Smart Spring was a torsional element, which had the baseline or initial stiffness ($k_i = k_1$) provided by a central torque tube. The final stiffness was obtained by adding the stiffness provided by three satellite structures containing stacked piezoelectric elements to the initial stiffness. An exploded view of the actuator structure is shown in Fig. 2. Thus, the Smart Spring prototype can be seen as a parallel arrangement of springs (or structural elements) acting in torsion about the central axis where $k_f = k_1 + k_2 = k_1 + 3\Delta k$, where $\Delta k$ is the torsional stiffness provided by each can about the central torque tube. The Smart Spring assembly without the front plate is shown in Fig. 3. Activation of the stacked piezoelectric elements in the actuator units controls the force applied to a front disk attached to the central torque tube as shown in Fig. 4. Therefore, the overall torsional stiffness of the system was controlled in a similar manner to that explained using the conceptual model in Fig. 1.

Controllable actuation of the active material actuators allows the Smart Spring prototype device to vary its total stiffness $k_i \leq k(t) \leq k_f$ within a broadband of frequencies, from DC to 200 Hz. Moreover, this stiffness change is effected with only small deformations of the actuators. This is a vast improvement over stiffness based passive vibration suppression techniques currently employed in helicopters, such as adding mass for blade tuning, that may only dampen rotor vibration at a specific frequency. High fre-

quency operation coupled with the simplicity of the concept makes the Smart Spring an attractive technique to be used for IBC in helicopter rotor vibration suppression.
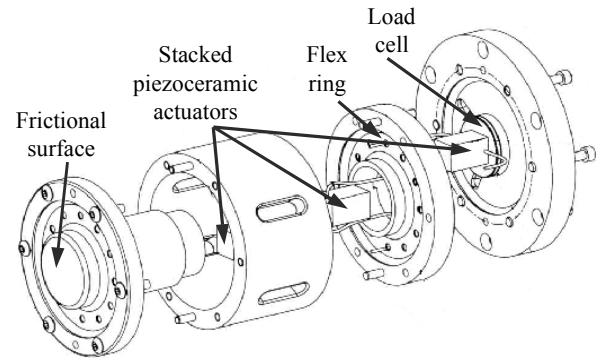


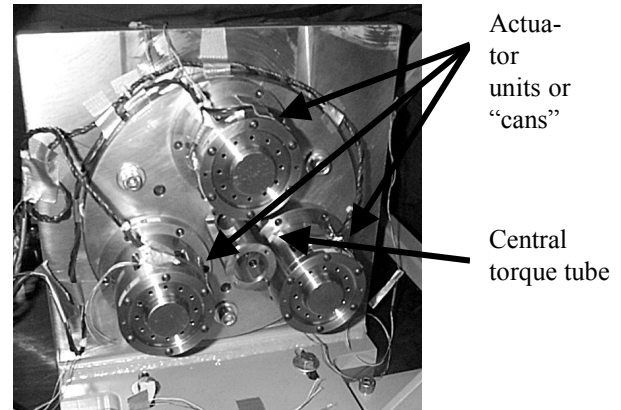Figure 2: Actuator unit ("can") assembly



Figure 3: Smart Spring proof-of-concept assembly without the front plate

PROOF-OF-CONCEPT HARDWARE

The Smart Spring proof-of-concept hardware included three actuator units or "cans" to apply a balanced load to an output plate. Interaction between the actuator units and the output plate generated the frictional forces necessary to engage the actuator units as active members to vary the torsional stiffness of the device. The primary stiffness of the device was tailored through the design of the central tubular torsion member that matched a typical blade torsional stiffness. The proof-of-concept hardware without the front output plate is shown in Fig. 3 and the complete assembly, with the front plate attached to a mechanical shaker, is shown in Fig. 4. The dynamic tests of the Smart Spring were previously reported [13].

The Smart Spring adaptive stiffness system consists of an array of sensors, such as accelerometers, a signal analysis processing computer, and stacked piezoelectric actuators. The sensors are embedded along the blade to provide the vibration information to the control computer, which analyzes these signals to determine the mode and amplitude of blade vibration. These data are used by the control logic to generate the control signal to the piezoelectric actuators. The forces generated by the controlled piezoceramic actuators adaptively vary the torsional stiffness at the blade root to suppress the rotor vibration.
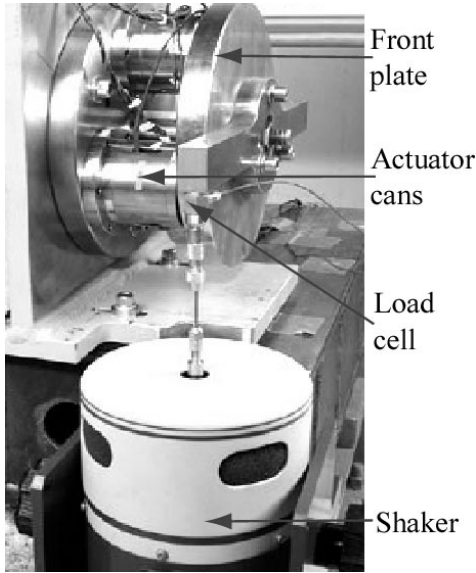


Figure 4: Complete Smart Spring proof-of-concept assembly undergoing shaker tests

It is worthwhile to point out that although the prototype of the Smart Spring was designed for simplicity to act only on the torsion degree of freedom of the blade, different designs can be devised, using the same principle, to actuate on the bending degree of freedom, which is fundamental for helicopter vibration suppression.

The primary advantage in the Smart Spring system, compared to other active material actuator based IBC systems, is that the Smart Spring does not rely on actuators to achieve high stroke and force simultaneously. Rather, the device only requires the actuators to produce micro displacement to generate the required actuation forces. The initial gap between the actuator surface and the structure is kept as low as possible to maximize the actuation force. This avoids problems of other IBC approaches that require high displacement and force simultaneously from the active material actuators. Furthermore, the stacked piezoceramic actuators are able to achieve the required micro displacements and actuation forces with voltages of less than 100 V. Safety in the system is enhanced by the use of low driving voltage.

Furthermore, the Smart Spring is more effective if placed near the blade root to alter its boundary conditions. Hence, the need to transmit high voltage electrical signals along the length of the blade is avoided, thereby reducing possible electromagnetic interference (EMI) problems that may be present in other IBC approaches.
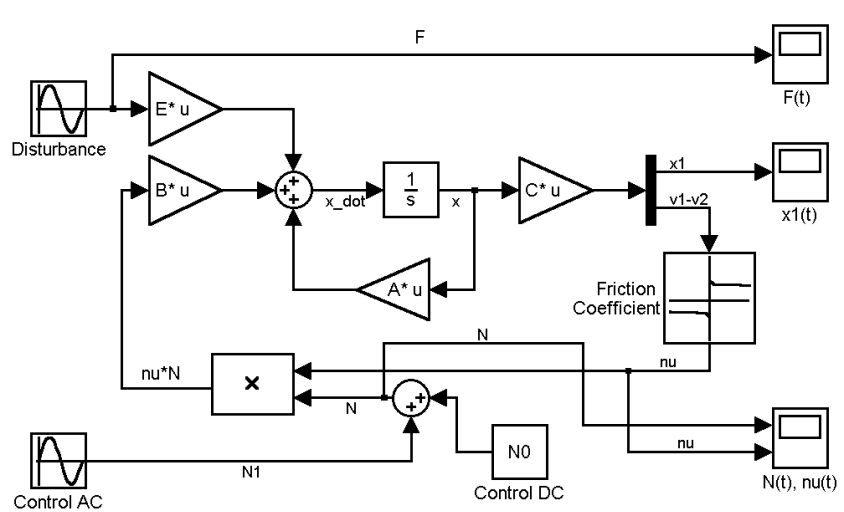


Figure 5: SIMULINK model for the Smart Spring. See Appendix for blocks definitions.

## SMART SPRING ANALYTICAL MODEL

The dynamic system shown in Fig. 1 is non-linear. It can be modeled by the following set of differential equations:

$$m_1 \ddot{x}_1 + k_1 x_1 = F(t) \mp v(t) N(t) \qquad (1)$$

$$m_2 \ddot{x}_2 + k_2 x_2 = \pm v(t) N(t) \qquad (2)$$

where the terms on the right hand side of the equations carry the upper sign if $\dot{x}_1 > \dot{x}_2$ and the lower sign if $\dot{x}_1 < \dot{x}_2$. In Equations (1) and (2), $v(t)$ denotes the kinetic friction coefficient between the two sliding sleeves, which is a non-linear function of the absolute relative speed $|\dot{x}_1 - \dot{x}_2|$ and the materials involved; here $t$ is the time and dots represent time derivatives. The simulation of the former equations can be simplified allowing the friction coefficient to absorb the switching sign on the right hand side of (1) and (2). This can be accomplished by assigning an odd extension to the function $v(t)$:

$$v(\dot{x}_2 - \dot{x}_1) = -v(\dot{x}_1 - \dot{x}_2) \qquad (3)$$

In this case, the equations of motion are rewritten using the upper sign only.

### The Concept of Impedance Adaptation

The SIMULINK block diagram depicted in Fig. 5 was used to simulate the non-linear system represented by (1), (2) and (3). Although the present characterization of the Smart Spring was performed using the conceptual model, the particular analysis of any TVA that can be identified as a Smart Spring will bear the same general characteristics.

In the helicopter rotor blade application, the Smart Spring device is placed near the blade root to dynamically alter the response of the blade by varying its dynamic stiffness or *impedance* at the root. The root of the blade is selected as the optimum location to dampen the rotor vibration because the loads are the highest and, accordingly, the Smart Spring has the greatest effect on the dynamic response of the structure.

In the following simulation, the parameters listed in Table 1 were used.

Table 1: Analytical Model Parameters

| parameter | value |
|---|---|
| $m_1$ | 1.90 kg |
| $k_1$ | $5.0 \times 10^4$ N/m |
| $m_2$ | 0.0633 kg |
| $k_2$ | $25.0 \times 10^4$ N/m |
| $v\left(|\dot{x}_1 - \dot{x}_2|\right)$ | steel/steel* |

*[14]

In Figs. 6 to 9, plots from an applied harmonic force, $F(t)$ versus displacement, $x_1(t)$ are presented on the left hand side of the figures for the control cases listed in the respective captions. The ratio of these two quantities is the dynamic stiffness or impedance, $k(t) = F(t)/x_1(t)$, seen by the structure attached to the Smart Spring. This structure is subjected to the boundary condition at the root defined by $k(t)$. The respective plots of $k(t)$ versus time are also presented as graphs on the right hand side of the figures. In the same plots, the static values of the stiffness, $k_i = k_1$ and $k_f = k_1 + k_2$ are shown as dashed lines.
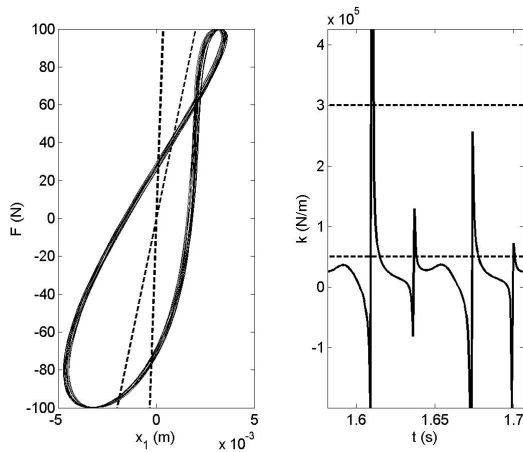


Figure 6: Smart Spring impedance characteristics for $F(t) = 100\sin(100t)$ N and $N(t) = 200 + 200\sin(100t)$ N
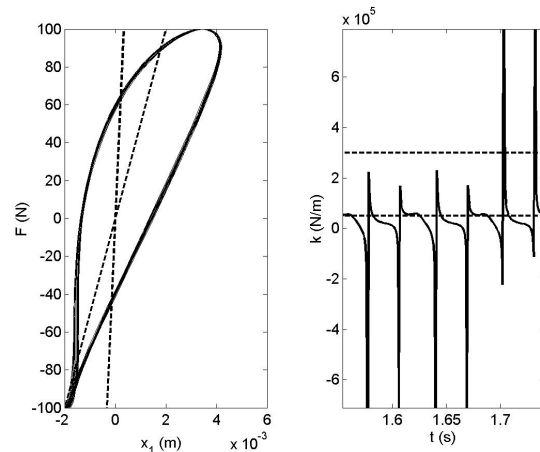


Figure 7: Smart Spring impedance characteristics for $F(t) = 100\sin(100t)$ N and $N(t) = 200 + 200\sin(100t + \pi)$ N
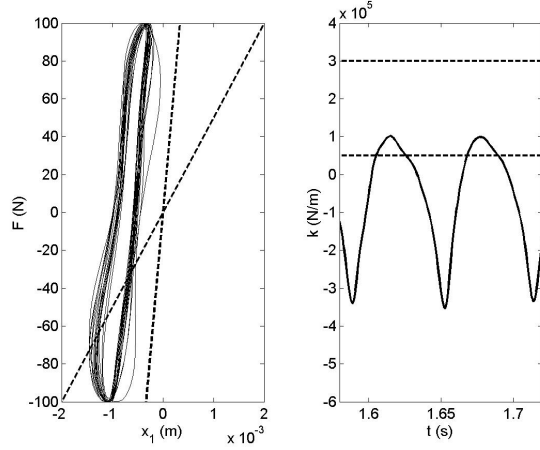
Figure 8: Smart Spring impedance characteristics
for $F(t) = 100\sin(100t)$ N and
$N(t) = 400 + 200\sin(100t)$ N



Figure 9: Smart Spring impedance characteristics
for $F(t) = 100\sin(250t)$ N and
$N(t) = 400 + 200\sin(250t)$ N

The Smart Spring is able to tailor its impedance according to the control signal, altering the structural boundary conditions. This is a function of the basic properties of the Smart Spring listed in Table 1 and the control signal, $N(t)$; namely, its frequency, magnitude and phase compared to the disturbance signal, $F(t)$. It is also important to point out that the static values of the stiffness that characterize the Smart Spring components are very distinct from the dynamic values observed by the structure attached to it. Therefore, an active control system may be synthesized to apply the "correct" control signal to the Smart Spring in order to *tailor the structure dynamic response* according to a control objective such as vibration suppression.

It is worthwhile to point out that $k(t)$ should in principle be periodic for a periodic control signal. However, due to the non-linear character of the system, introduced in the present model by friction, this periodicity is only partially achieved. This can easily be observed from the plots because the hysteretic loops change slightly from one cycle to the next. In addition to this behavior, actual hardware factors such as temperature variations and contact surface wear, are expected to affect $v(t)$ greatly, suggesting that the control algorithm must be adaptive.

## CONTROL ALGORITHM DEVELOPMENT

An algorithm was developed to adaptively control the piezoelectric stacked actuators to alter the blade dynamic torsional stiffness in real-time to suppres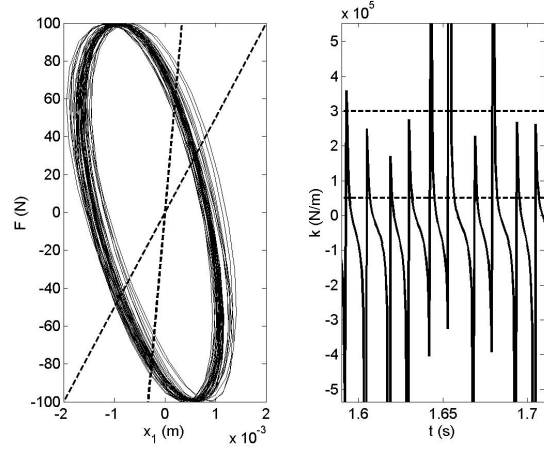s the rotor vibration. Both active and adaptive control algorithms were developed and implemented on a Digital Signal Processor (DSP) platform and tested using the Smart Spring proof-of-concept hardware model.

## Active Control Strategy

In the preliminary phase of the controller development, an active control algorithm was implemented. A sine signal was used to drive the mechanical shaker to simulate a harmonic vibration source from the rotor blade. The vibration from the blade was trimmed by actively altering the stiffness of the Smart Spring at the frequency of the excitation force. While keeping the magnitude of the force generated by the piezoceramic actuators constant, shifting the phase of the actuator force with respect to the excitation vibration resulted in an appreciable variation in vibration suppression. This active controller achieved significant suppression of the excitation vibration when the Smart Spring stiffness was varied out of phase by 90° from the excitation vibration. This suggested that an adaptive control algorithm could greatly improve the vibration suppression performance of the Smart Spring.
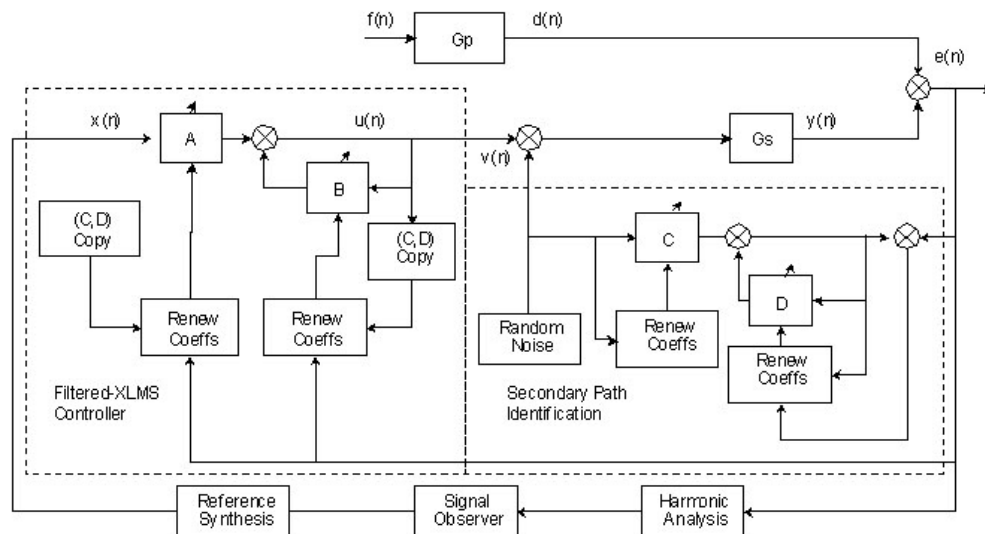
## Adaptive Control Strategy

As discussed in a previous section, the Smart Spring device exhibits non-linear dynamic characteristics due to the operation of piezoceramic actuators and the frictional forces between the mating surfaces. To optimize the performance in this non-linear system, a Filtered-X LMS adaptive feed-forward algorithm was

chosen as the closed loop controller. A block diagram of the controller is shown in Fig. 10.

The disturbance signal, $f$ is passed through the transfer function matrix, $Gp$, which represents the primary path of the system, producing a vector of disturbance signal, $d$. A secondary path between actuator input signal, $u$ and output, $y$ flows through the matrix $Gs$. The output error signal measured by a displacement probe is here denoted by $e$. An Infinite Impulse Response (IIR) filter was used to produce the control signal to the actuators although the secondary path is in the discrete time domain.

The filter identification algorithm was implemented on-line and real-time to take the time-varying factors into account [15]. This requires the identification process to occur in parallel with the control process. However, the performance achieved in such controllers is sensitive to the strength of the training random signal. The training signal strength must be high for good system identification. On the other hand, the training signal strength must also be as low as possible to implement an effective control process. These contradicting requirements for training signal strength for on-line identification have been proven to be difficult in many cases. Furthermore, the computational speed required to simultaneous real-time system identification and control is high, especially for high frequency. Under the assumption of slowly varying plant model coefficients and zero initial conditions,

off-line identification was used for the secondary path identification for the initial tests [16]. However, real-time system identification was recognized as a requirement to be implemented during aerodynamic loading tests on the Smart Spring system.

The reference signal is a very important factor for the successful performance of a feed-forward adaptive controller. In most cases, this is achieved by measuring the primary disturbance with a suitable reference sensor. This technique is effective for both broadband (random) and narrow band (periodic) disturbances with some limitations. In this work, the wave synthesis technique was used to overcome the difficulty of providing a stable reference signal [15]. The wave synthesis technique assumes a slowly varying process where the next cycle has the same waveform as the current cycle. This technique is appropriate for the range of frequencies associated with rotary-wing problems.

The vibration from the blade was suppressed with a higher-order filter with multiple notches. An auxiliary sensor was used to implement this approach. The output from the sensor was first analyzed to determine the frequencies and amplitudes of the higher harmonic components. Next, the reference input was synthesized as a sum of the main sinusoidal components. In order to accommodate the changes in the flight conditions, the analysis was performed on-line to update the harmonic frequencies without requiring



Figure 10: Filtered-X LMS control algorithm

new identification. This reference signal, based on a sum of sinusoidal components, was applied to an adaptive filter in order to define a notch at each reference frequency to provide effective vibration cancellation.

## SMART SPRING TESTING

The Smart Spring was tested using a mechanical input as well as in the wind tunnel. The mechanical tests were conducted on the Smart Spring proof-of-concept model at different single frequency excitations produced by the mechanical shaker. Mechanical tests proved the ability of the Smart Spring to achieve active impedance control of the structure to suppress the vibration significantly [17]. Wind tunnel tests of the Smart Spring proof-of-concept hardware were also conducted to evaluate the performance of the device in a more representative rotor blade aerodynamic loading environment. This test was the first in a series of tests designed to evaluate the capability of the Smart Spring concept for IBC application.
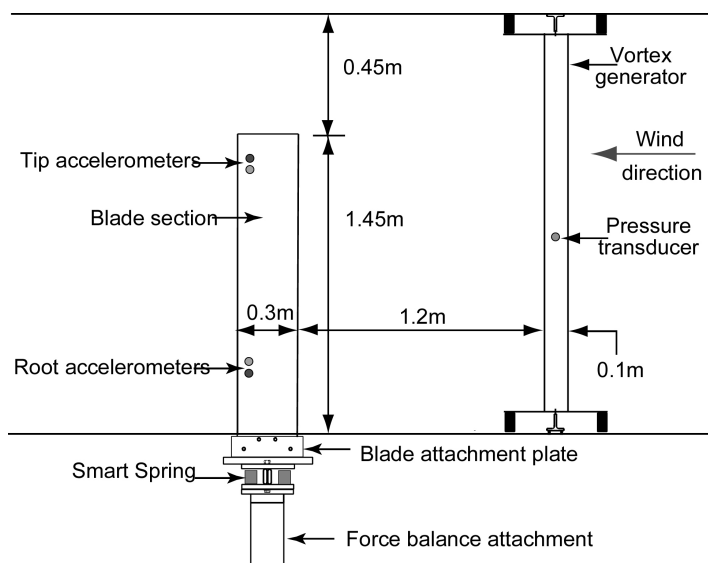
### Wind Tunnel Test Set-up

Fixed blade tests were conducted in the low speed wind tunnel facility at the Institute for Aerospace Research of the National Research Council Canada. Test section was 1.9 m x 2.7 m x 5.2 m with a contraction ratio of 9:1. The Smart Spring was attached to one end of a 1.45 m blade section with a 0.3 m

chord in a cantilever configuration to perform damping augmentation of the blade vibration. The blade and the Smart Spring assembly were installed on the wind tunnel force balance such that the Smart Spring device was underneath the floor. A 0.1 m square tube was installed 1.2 m upstream from the leading edge of the blade to produce vortices. The shredded vortices were characterized using the measurements from a pressure transducer installed on the side of the square tube. Accelerometers were placed on the trailing edge of the blade section near the root and the tip to measure the vibratory acceleration and displacement on the blade. The diagram of the wind tunnel test set up is shown in Fig. 11.

### Wind Test Procedure

The wind tunnel tests were conducted with zero angle-of-attack to minimize the lift (and bending) generated by the blade. It was important to minimize the bending mode of the blade vibration because the Smart Spring proof-of-concept hardware was designed to suppress only the torsional vibration mode. The wind speed and the dimension of the vortex generator determined the fundamental vibratory frequency. The pressure transducer signal from the vortex generator was used to identify the excitation characteristics of the blade. The accelerometer signals from the blade root and tip were measured to determine the blade response. Increase in the DC voltage of the actuators only increases the stiffness of the Smart Spring. However, introduction of an AC voltage through a controller enables impedance control of the Smart Spring. The actuator units were con-



Picture of the wind tunnde test set-up

Figure 11: Smart Spring wind tunnel tests setup

trolled using an active controller as well as an adaptive controller. The active controller engaged the actuator units with a specific phase offset with respect to the excitation. In a second test, a more complex adaptive controller adaptively engaged the actuator units with optimum phase offset and amplitude to suppress vibration.

## Wind Tunnel Test Results

The 10 m/s wind speed with 0.1 m vortex generator produced an excitation frequency of 12.7 Hz. FFT analyses of the blade root displacement are shown in Figs. 12 and 13 for active and adaptive control test conditions. The baseline operating condition of the actuators in the proof-of-concept hardware model was 0 Vdc and this produced the highest vibratory displacement.

Figure 12 shows that increasing the actuator voltage to 50 Vdc and 90 Vdc only increased the stiffness in the Smart Spring, which, in turn, reduced the vibratory displacement at the blade root by 50% and 60%, respectively. A higher reduction of 72% in vibratory displacement was achieved by active impedance control of the Smart Spring with the use of a 50 Vdc+40 Vpp voltage with 225°-phase offset.
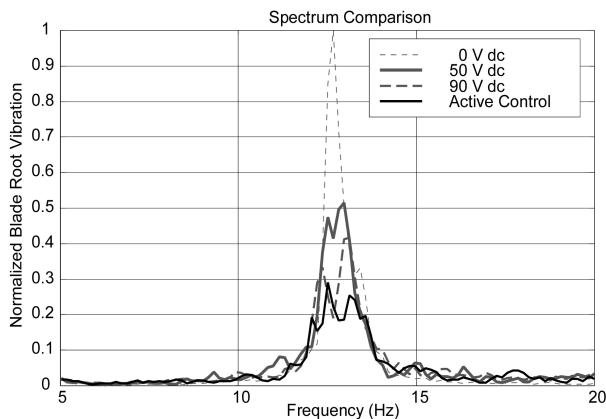


Figure 12: Active Control Results

Initial tests with the adaptive controller, depicted in Fig. 13, also demonstrated significant vibration reduction. The results indicate that the adaptive control achieved 50% reduction in the vibration with 50 Vdc +22 Vpp. Due to the highly random nature of the perturbation frequency produced by the vortex generator, the adaptive controller used a 12.7 Hz synthesized signal as a reference instead of the actual perturbation. Higher vibration suppression could be achieved if the full voltage range of 45 Vpp were used. How-

ever, the controller due to the randomness of the perturbation frequency did not enable this. Modifications in the adaptive controller may be required to improve performance.
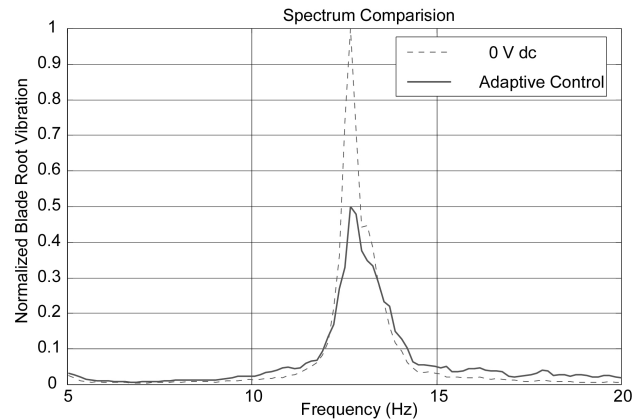


Figure 13: Adaptive Control Results

## CONCLUSIONS

The Smart Spring provides a unique approach to helicopter IBC vibration reduction. By altering the structural response of the blade rather than the aerodynamic forces, this concept promises to overcome some of the significant problems encountered in other IBC concepts. A proof-of-concept Smart Spring hardware model has been designed, built, and tested in wind tunnel. Results from the tests provide positive support of the viability of the approach.

## REFERENCES

1. Lemnios, A. Z., and Nettles, W. E., "The Controllable Twist Rotor Performance and Blade Dynamics," Proceedings of the 28th Annual Forum of the American Helicopter Society, 1972.

2. Giurgiutiu, V., "Recent Advances in Smart-Material Rotor Control Actuation," AIAA-2000-1709, Proceedings of the 41st AIAA Structures, Structural Dynamics and Materials Conference, Atlanta, GA, April 2000.

3. Straub F. K., "A Feasibility Study of Using Smart Materials for Rotor Control," Proceedings, 49th Annual Forum of the American Helicopter Society, St. Louis, MO, May 1993.

4. Prechtl, E. F., and Hall, S. R., "Closed-Loop Vibration Control Experiments on a Rotor with Blade Mounted Actuation," AIAA-2000-1714, Proceedings of the 41st AIAA Structures, Structural Dynamics and Materials Conference, Atlanta, GA, April 2000.

5. Straub, F. K., et al, "Smart Material Actuated Rotor Technology – SMART," AIAA-2000-1715, Proceedings of the 41st AIAA/SDM Conference, Atlanta, GA, 3-6 April 2000.

6. McCloud, J. L., and Weisbrich A. L., "Wind-Tunnel Results of a Full-Scale Multi-Cyclic Controllable Twist Rotor," Proceedings, 34th Annual Forum of the American Helicopter Society, 1978.

7. Rodgers, J. P., and Hagood, N. W., "Hover Testing of 1/6 Mach-Scale CH-47D Blade with Integral Twist Actuation," Presented at 9th International Conference on Adaptive Structures and Technology, Cambridge, MA, 1998.

8. Shin, S. J., and Cesnik, C. E. S., and Wilbur, M. L., "Dynamic Response of Active Twist Rotor Blades," AIAA-2000-1711, Proceedings of the 41st AIAA/SDM Conference, Atlanta, GA, April 2000.

9. Wickramasinghe, V. K., Hagood, N. W., "Performance Characterization of Active Fiber Composite Actuators for Helicopter Rotor Blade Applications," Proceedings of SPIE 9th Smart Structures and Materials Symposium, San Diego, CA, 2002.

10. Nitzsche, F., Lammering, R. and Breitbach, E., 1993, "Can Smart Materials Modify the Blade Root Boundary Conditions to Attenuate Helicopter Vibration?" Fourth International Conference on Adaptive Structures, November 2-4, 1993, Breitbach, E. J., et al. Editors, Technomic Publishing Co., 1994, pp. 139-150.

11. Nitzsche, F., "Aeroelastic Analysis of Helicopter Rotor Blade with Active Impedance Control at the Root," Canadian Aeronautics and Space Journal, Vol. 47 No. 1, pp. 7-16, March 2001.

12. Nitzsche, F., Grewal, A., Zimcik, D. G., "Structural Component Having Means for Actively Varying its Stiffness to Control Vibrations" US patent 5,973,440, October 1999 and European Patent EP-996570-B1, 2001.

13. Zimcik, D. G. et al., "Smart Spring Concept for Active Vibration in Helicopters," Structures and Materials II, Paper No. 3, AHS International 58th Annual Forum, Montreal, Canada, June 2002.

14. Avallone, E. A. and Baumeister III, T., *Mark's Standard Handbook for Mechanical Engineers,* 10th Edition, McGraw Hill, p. 3-22.

15. Kuo, S. M., and Morgan, D. R., Active Noise Control Systems, John Wiley & Sons, 1996.

16. Grewal, A., Zimcik, D. G., "Feed-forward Piezoelectric Structural Control: An Application to Aircraft Cabin Noise Reduction," Journal of Aircraft, Vol. 38, No. 1, pp. 164-173, Jan-Feb 2001.

17. Zimcik, D. G. et al., "Smart Spring Concept for Helicopter Vibration and Noise Control," 23rd Congress of the International Council of the Aeronautical Sciences, Paper No. 0406, Toronto, Canada, September 2002 (to be published).

## APPENDIX

In the SIMULINK block diagram shown in Fig. 5, the following set of non-linear equations were simulated:

$$\{\dot{x}\} = [A]\{x\} + \{B\}v(t)N(t) + \{E\}F(t)$$
$$\{y\} = [C]\{x\}$$

where

$$\{x\} = \begin{Bmatrix} \dot{x}_1 \\ x_1 \\ \dot{x}_2 \\ x_2 \end{Bmatrix} \quad [A] = \begin{bmatrix} 0 & -k_1/m_1 & 0 & 0 \\ 1 & 0 & 0 & 0 \\ 0 & 0 & 0 & -k_2/m_2 \\ 0 & 0 & 1 & 0 \end{bmatrix}$$

$$\{B\} = \begin{Bmatrix} 1/m_1 \\ 0 \\ 0 \\ 0 \end{Bmatrix} \quad \{E\} = \begin{Bmatrix} -1/m_1 \\ 0 \\ 1/m_2 \\ 0 \end{Bmatrix} \quad \{y\} = \begin{Bmatrix} x_1 \\ v_1 - v_2 \end{Bmatrix}$$

$$[C] = \begin{bmatrix} 0 & 1 & 0 & 0 \\ 1 & 0 & -1 & 0 \end{bmatrix}$$

and $v(t)$ was obtained via the Look-up Table block in SIMULINK.